On the Extraction of Long-living Features in Unsteady Fluid Flows

Jens Kasten[1], Ingrid Hotz[1], Bernd R. Noack[2], and Hans-Christian Hege[1]

[1] Zuse Institute Berlin (ZIB), {kasten;hotz;hege}@zib.de
[2] Berlin Institute of Technology MB1, Bernd.R.Noack@tu-berlin.de

Abstract. This paper proposes a Galilean invariant generalization of critical points of vector field topology for $2D$ time-dependent flows. The approach is based upon a Lagrangian consideration of fluid particle motion. It extracts long-living features, like saddles and centers, and filters out short-living local structures. This is well suited for analysis of turbulent flow, where standard snapshot topology yields an unmanageable large number of topological structures that are barely related to the few main long-living features employed in conceptual fluid mechanics models. Results are shown for periodic and chaotic vortex motion.

1 Introduction

With increasing computational power and advancement in experimental techniques, the focus in flow visualization has moved from steady to unsteady fields. The demands for analysis and visualization tools have changed accordingly. Many successful methods for steady fields, such as extraction of vector field topology, only provide an incomplete view on unsteady phenomena.

There are two viewpoints for describing a flow, dependent on the choice of independent variables. The Eulerian view assigns dynamic properties to fixed points in space, while the Lagrangian view assigns these to moving fluid parcels; the dynamic equations describe changes that occur to a fluid particle along its trajectory. This view corresponds to a natural extension of particle mechanics. Both views can be transformed into each other and offer different perspectives onto the flow behavior; for more details see [Pan05]. Especially for unsteady flows, it is important to provide analysis tools offering both perspectives.

Vector field topology has permeated fluid dynamics since entering the scientific field [TP82]. It has significantly supported the development of conceptual flow models for steady flows or snapshots of time dependent flows. Standard vector field topology is based on streamline behavior and thus is appropriate to capture snapshot features. Pathline or streakline related features are not represented. Furthermore, topological features are not invariant under *Galilean transformations*. These are transformations between two frames of reference that differ by a constant relative motion. The distinguished points in vector field topology are fixed points that exhibit zero velocity. Thus, choosing a suitable Galilean transformation any location can be turned into a feature point. Additional practical limitations result from the complexity of the topological skeleton and its

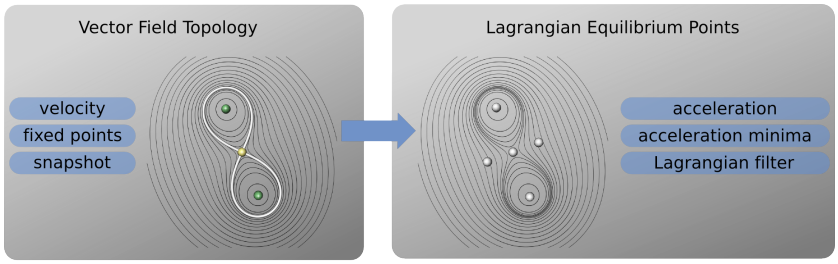

Fig. 1. Correspondences between critical points from standard vector field topology and Lagrangian equilibrium points. Displayed are the respective distinguished points with streamlines providing context.

high feature density. Distinguishing long-living structures from short-living incoherent structures is not easy.

Some of these problems have been tackled by the introduction of Lagrangian coherent structures. These long-living features can be extracted in a number of ways, for example by analysis of the *Finite Time Lyapunov Exponent* field [Hal02]. This measure characterizes the separation of particles over time, providing a Galilean invariant Lagrangian view. Coherent features are depicted as ridges of high separation. Center or vortex-like features are not considered by this approach, since nearly no separation can be observed here.

This paper follows a different approach to Lagrangian coherent structures, motivated by two points: 1) The concept of critical points is successful, but its applicability to unsteady flow fields is limited. We introduce an unsteady analogon to the zero velocity definition of critical points. In the steady case, particles at fixed points have zero acceleration, which is a Galilean invariant property. Generalizing this behavior to unsteady fields, particles with low acceleration compared to their neighbors become particles of interest. We call these features *Lagrangian equilibrium points* (LEP). 2) Fluid flow researchers are mainly interested in the dominant structures that mainly influence the flow behavior. These interesting and influential features usually exist over some period of time. The time a particle exhibits a given property becomes a basic component of the analysis. In the proposed approach short-living structures are filtered out by a lifetime parameter leaving only salient features. We consider the extracted features to be a first building block of a *Finite Time Topology* (FTT). We verify the significance of this approach by applying it to basic well-known flow structures such as a mix of Oseen vortices. We limit our considerations to unsteady 2D fields and leave an extension to 3D fields for future work.

2 Related Work

Streamline topology was introduced by Tobak and Peake [TP82] to the flow community and by Helman and Hesselink [HH89,HH91] to the visualization community a few years later. In this early work, they define the concept of fixed points and integral curves connecting these, thereby building a topological skeleton. Af-

terwards, many extensions like simplifications and tracking algorithms have been published. We refer to the survey paper [LHZP07] and the references therein.

Appropriate vortex definitions and extraction methods are crucial for the understanding of complex flows. A variety of scalar quantities have been introduced to extract vortex regions. Two of the most commonly used vortex identifiers are Q [Hun87] and λ_2 [JH95]. Both measures are based on the Jacobian matrix of the flow field and are Galilean invariant. Geometrical approaches using streamline curvature for locating vortices [SP00] are not Galilean invariant. Other methods employ the parallel vectors operator [PR00] for computing global line-like features, such as vortex cores.

Most of the methods mentioned above are based either on streamlines or the Jacobian matrix. They are well suited for analysis of single time-slices but not for characteristics of unsteady flow fields. Thus, more attention has been paid to methods based on pathline analysis, representing the Lagrangian point of view. Theisel et al. [TWHS05] have presented an extension of streamline topology to pathlines. Weinkauf et al. [WSTH07] have generalized the parallel vectors method to detect cores of swirling motion. Fuchs et al. [FPS+08] accumulate Eulerian quantities along pathlines to add a Lagrangian view. Similarly, Shi et al. [STW+08] explore the dynamical process of a flow by averaging the kinetic energy and momentum along pathlines.

Other features have also been identified as interesting by fluid flow researchers and have subsequently found their way into flow visualization. Haller, for instance, has introduced an analytical criterion for finite-time attracting and repelling material surfaces [Hal01a]. A further advancement has been the introduction of the Finite Time Lyapunov Exponent (FTLE) [Hal02], which is a scalar quantity indicating the separation rate of infinitesimal close particles. Using ridge extraction [SP07], Lagrangian coherent structures can be captured. Garth et al. [GGTH07] have presented a computational less expensive, adaptive method to extract FTLE ridges.

3 Motivation

3.1 Acceleration and Lagrangian Equilibrium Points

The goal of this section is to explain the considerations that finally leads to the definition of *Lagrangian equilibrium points*. Vector field topology defines critical points as fixed points, as shown on the left hand side of Fig. 1. This definition does not satisfy the requirement of Galilean invariance. This fact motivates the investigation of alternative concepts for "distinguished points". In the following, let $\mathbf{v}$ be a flow field. As a technical requirement it is assumed that its spatial and time derivatives are bounded. Our starting point is the observation that for steady fields the particle acceleration at fixed points is equal to zero. Furthermore, particle acceleration is a Galilean invariant entity, see Appendix. The particle acceleration $\mathbf{a}$ is the material derivative of the field $\mathbf{v}$, i.e. the acceleration in a space-time point $(\mathbf{x}, t)$ is given by

$$\mathbf{a}(\mathbf{x}, t) = D\mathbf{v}/Dt = \partial_t \mathbf{v}(\mathbf{x}, t) + (\mathbf{v}(\mathbf{x}, t) \cdot \nabla)\, \mathbf{v}(\mathbf{x}, t), \tag{1}$$

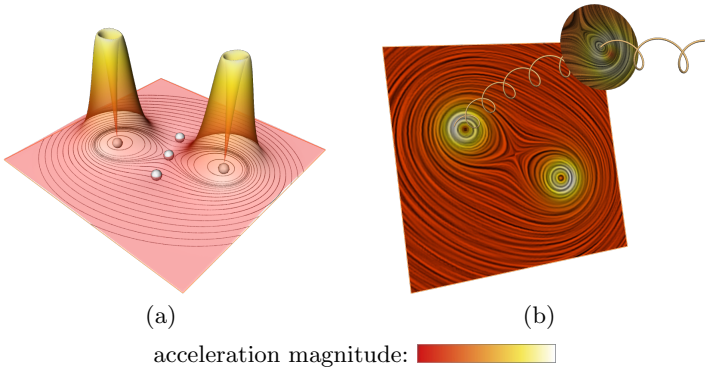

Fig. 2. Visualization of two co-rotating Oseen vortices in two dimensions (a) The acceleration magnitude of one time-slice is shown as a color-coded heightfield. The extracted points are the acceleration minima – which include fixed points. (b) The pathline of a particle seeded in one time-slice is displayed. The time is depicted as third dimension. The relative behavior of the flow field in the neighborhood of this particle at a later point in time is displayed on a surrounding circular disk. The acceleration magnitude is color coded in the line integral convolution (LIC) images of the flow field.

where ∂_t is the partial derivative with respect to t and ∇ the spatial gradient, i.e. (∂_x, ∂_y) for the two-dimensional case. The squared magnitude of the acceleration $\mathbf{a}$ defines a scalar field in the space-time domain by

$$\|\mathbf{a}\|^2 = \|\partial_t \mathbf{v}\|^2 + 2\,\partial_t \mathbf{v} \cdot ((\mathbf{v} \cdot \nabla)\,\mathbf{v}) + \|(\mathbf{v} \cdot \nabla)\,\mathbf{v}\|^2. \tag{2}$$

For steady fields the partial time derivative vanishes, $\partial_t \mathbf{v}(\mathbf{x}, t) = 0$, resulting in

$$\mathbf{a}(\mathbf{x}) = D\mathbf{v}/Dt = (\mathbf{v}(\mathbf{x}) \cdot \nabla)\,\mathbf{v}(\mathbf{x}). \tag{3}$$

It follows that at fixed points, where $\mathbf{v}$ is zero, the acceleration also equals zero and its magnitude $\|\mathbf{a}\|$ takes its *minimum value* 0, cf. Fig. 2(a). Thus, the set of fixed points is a subset of the zeros of the acceleration field.

The next step is to look at time-dependent vector fields. It turns out that for unsteady fields it is not sufficient to consider points where the acceleration of a fluid particle is equal to zero. In general unsteady flow fields, structures like centers and saddles evolve over time, and thus the acceleration does not vanish. This fact also follows from Eq. (2), since at fixed points the squared magnitude of the particle acceleration equals $\|\partial_t \mathbf{v}\|^2$, which does not vanish in general. However, the acceleration at fixed points is not zero but is still small compared to its neighborhood for time-dependent fields. This allows us to relax the condition of a vanishing acceleration to a less strong requirement, the *minimality* of $\|\mathbf{a}\|^2$.

As an illustrating example, Fig. 3 shows a steady and a convecting version of the Stuart vortex. For a detailed discussion on Stuart vortices see Panton [Pan05]. Note that convection adds a non-stationary component to the steady field due to the moving frame of reference. For both fields the same acceleration minima are detected, while the location of fixed points are different.

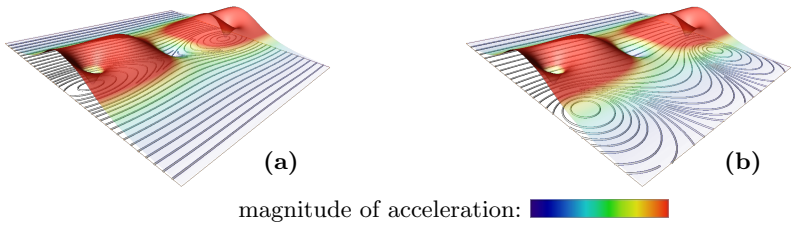

Fig. 3. Stuart vortices in two inertial frames of references: (a) vortices at rest, (b) convecting vortices such that the velocity at the bottom becomes zero. Heightfield and color represent the absolute value of the particle acceleration. The acceleration field is the same in both cases, while the streamline patterns, observed from different inertial systems, differ.

As a result, acceleration and its minima are used as key features for unsteady flow fields. In the following, space-time points $(\mathbf{x_0}, t_0)$ where $\|\mathbf{a}(\mathbf{x_0}, t_0)\|$ takes a local minimum in space are called *Lagrangian equilibrium points*.

3.2 Feature Lifetime and Long-Living Flow Structures

In real-world datasets the high density of features often complicates a proper analysis. An appropriate filter mechanism differentiating between important and unimportant structures can ease this problem. Since fluid flow researchers are mainly interested in long-living structures, the lifetime of features is a meaningful filter criterion. Thus, special attention is paid to particles that carry the minimality property of $\|\mathbf{a}\|$ for at least a small period of time. The proposed feature identifier makes use of the 'feature lifetime' in two ways: (i) Considering and averaging the acceleration magnitude along pathlines over a lifetime interval reinforces the Lagrangian perspective of the approach. (ii) An explicit *feature lifetime* filter selecting particles that stay in a feature state a certain time period enables the extraction of long-living features.

4 Proposed Feature Extraction Technique

4.1 Method

The center of a Lagrangian point of view is the behavior of particles, represented by pathlines and the evolution of flow properties along these lines. Each pathline is identified by its initial position $\mathbf{x}_0$ at time t_0 and the corresponding trajectory $\mathbf{s}(t, \mathbf{x}_0, t_0) = \mathbf{s}$ depending on the time parameter t. The contribution of a pathline to a certain feature $\mathcal{F}$ is measured using a *feature importance* $I_{\mathcal{F}}$; it is defined as the average of a scalar *feature identifier* $f(\mathbf{x}, t)$ over some feature time span $[t_{\min}(\mathbf{x}_0, t_0), t_{\max}(\mathbf{x}_0, t_0)]$

$$I_{\mathcal{F}}(\mathbf{x}_0, t_0) = \frac{1}{t_{\max}(\mathbf{x}_0, t_0) - t_{\min}(\mathbf{x}_0, t_0)} \int_{t_{\min}(\mathbf{x}_0, t_0)}^{t_{\max}(\mathbf{x}_0, t_0)} f\left(\mathbf{s}(t, \mathbf{x}_0, t_0), t\right)^2 dt. \quad (4)$$

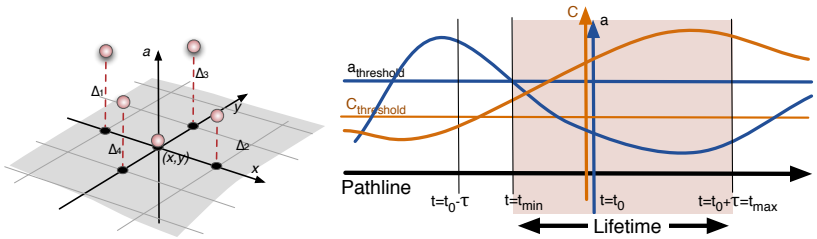

(a) (b)

Fig. 4. (a) The minimality of the acceleration can be measured by the Laplacian of the scalar field $\|a\|$, which can be computed by central differences. (b) Definition of a feature's lifetime along a pathline. The parameter $t_{\min}$ is determined by the acceleration threshold and $t_{\max}$ by the maximum lifetime window.

The choice of the parameters $t_{\max}(\mathbf{x}_0, t_0)$ and $t_{\min}(\mathbf{x}_0, t_0)$ is crucial, since they determine the time range of influence to the local value. They are determined by the time a pathline exhibits a certain feature state. Thus, they depend on the feature considered and are derived for each pathline segment. The feature lifetime is defined as

$$T_{\mathcal{F}}(\mathbf{x}_0, t_0) = t_{\max}(\mathbf{x}_0, t_0) - t_{\min}(\mathbf{x}_0, t_0). \tag{5}$$

More specifically, for *Lagrangian equilibrium points* the feature identifier is the acceleration magnitude $a(\mathbf{x}, t) = \|\mathbf{a}(\mathbf{x}, t)\|$. The lifetime parameters $t_{\min}(\mathbf{x}_0, t_0)$ and $t_{\max}(\mathbf{x}_0, t_0)$ are based on three quantities: acceleration magnitude a, a minimality measure of the acceleration C_{a}, and a maximum lifetime window τ. To measure the minimality the differences of $a(\mathbf{x}_0, t_0)$ at neighboring points are averaged in the four main directions: $C_{\mathrm{a}} = 1/4 \sum_{i=1}^{4} \Delta_i$, where $\Delta_i, i = 1, .., 4$ are defined in Figure 4(a). $C_{\mathrm{a}} > C_{\mathrm{threshold}}$ indicates that a particle has low acceleration compared to its neighbors.

A maximum lifetime window $[t_0 - \tau, t_0 + \tau]$ restricts the values of $t_{\max}$ and $t_{\min}$. Since saddle and vortex regions exhibit different characteristic behavior, the parameter τ can be chosen for each of these structures separately. Possible criteria to distinguish saddle and vortex regions can be based on the instantaneous Jacobian matrix and its characteristics, Q, λ_2 or the Lagrangian approach of Haller [Hal01b]. In the following the Jacobian matrix is used.

Finally, the lifetime parameters are defined as (cf. Figure 4(b))

$$\begin{aligned} t_{\min}(\mathbf{x}_0, t_0) = \min(t' \in [t_0 - \tau, t_0] \mid \forall t \in [t', t_0] : \\ a(\mathbf{s}(t, \mathbf{x}_0, t_0), t) \leq a_{\mathrm{threshold}} \text{ and} \\ C_{\mathrm{a}}(\mathbf{s}(t, \mathbf{x}_0, t_0), t_0) \geq C_{\mathrm{threshold}}), \end{aligned} \tag{6}$$

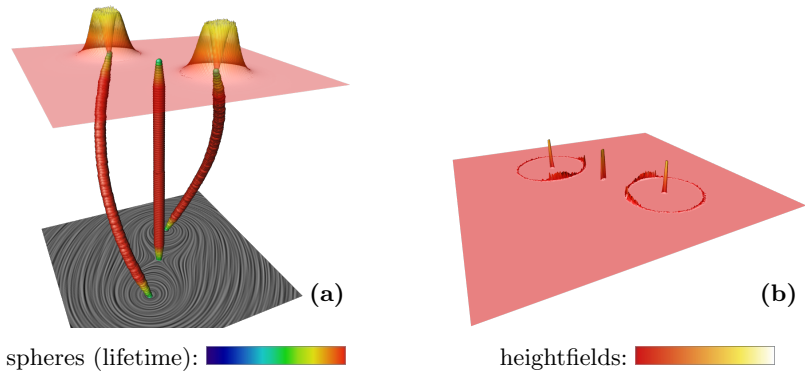

Fig. 5. Illustration of the *Lagrangian equilibrium point* concept for two co-rotating Oseen vortices. The color-coded heightfield represents: (a) integrated acceleration, (b) and lifetime for the last time step.

and

$$\begin{aligned} t_{\max}(\mathbf{x}_0, t_0) = \max(t' \in [t_0, t_0 + \tau] \mid \forall t \in [t_0, t'] : \\ a(\mathbf{s}(t, \mathbf{x}_0, t_0), t) \leq a_{\text{threshold}} \text{ and} \\ C_{\text{a}}(\mathbf{s}(t, \mathbf{x}_0, t_0), t_0) \geq C_{\text{threshold}}), \end{aligned} \tag{7}$$

If one of the criteria is not fulfilled at particle position $\mathbf{x}_0$ and time t_0, the feature lifetime is defined as zero and $t_{\max}(\mathbf{x}_0, t_0) = t_{\min}(\mathbf{x}_0, t_0) = t_0$; furthermore, the acceleration is not averaged over the lifetime and the resulting importance value is set to the square of the local acceleration magnitude.

Subsequently, feature candidates are extracted by searching minima in the resulting scalar importance field $I_{\mathcal{F}}$. Finally, a filtering with the extracted lifetime distinguishes important and unimportant features.

4.2 Implementation

The input to the algorithm is a 2D vector field defined on a sample grid. The algorithm consists of three main steps: integration of the acceleration values, extraction of the minimum points and filtering of these points with the lifetime.

Integration. The first step is the determination of the lifetime parameters, according to Eqs. (5), (6) and (7). A suitable threshold value for a is extracted by analyzing the acceleration characteristics of the first time-slice of the dataset. In this exploratory work it is simply set to ten percent of the maximum value. The threshold C_a has to be set a little above zero, to avoid setting a long lifetime for regions with low acceleration at all. For each discrete point $(\mathbf{x}_0, t_0)$, a backward search in time on the trajectory $\mathbf{s}$ determines $t_{\min}(\mathbf{x}_0, t_0)$. The lifetime criteria at each sample step on $\mathbf{s}$ is tested until either one of the thresholds is violated, or the maximum time window or the domain boundary is reached. Then, the feature importance is computed according to Eq. (4). For numerical integration,

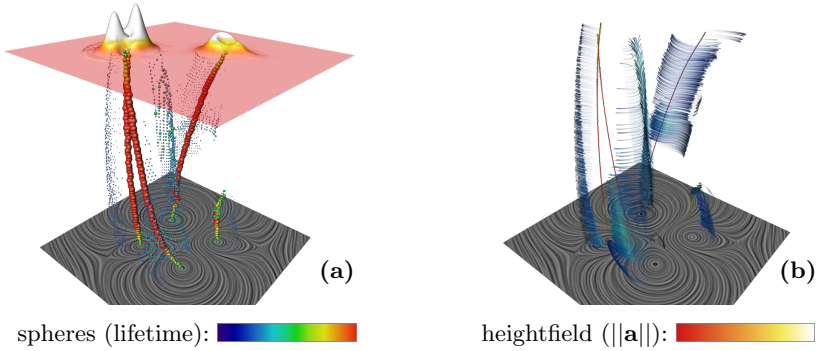

Fig. 6. (a) Extraction of features for a motion of six Oseen vortices. Since particles leave the saddle regions quickly, the saddles do not emerge as prominently as the vortex cores. The integration windows of 0.3 in each direction are too large for particles passing through the saddle in the center. In comparison, all other long-living structures such as the vortex cores are extracted effectively. The heightfield represents the integrated acceleration. (b) Visualization of the feature lifetime. The illuminated pathline segments show the interval of the lifetime used for the integration of the acceleration. Pathlines seeded in vortex-like feature points are long centerlines, while pathlines seeded in saddle-like feature points diverge rapidly.

a *Runge-Kutta* integrator RK4(3) with adaptive step-size control is used. After the starting point $t_{\min}$ for the forward integration is found, the accumulation of the acceleration magnitude along $\mathbf{s}$ is started. The integration is terminated if one of the lifetime criteria is not fulfilled. Then, the resulting values are normalized by the factor $1/T_{\mathcal{F}}(\mathbf{x}_0, t_0)$ and both lifetime $T_{\mathcal{F}}(\mathbf{x}_0, t_0)$ and importance measure $I_{\mathcal{F}}$ are stored as scalar fields.

Extraction. Feature candidates are extracted by searching local minima in the importance field I using a discrete neighbor analysis. Alternatively, other methods like the watershed transformation [Soi99] could be used for locating local minima.

Filtering. After these initial feature candidates are found, the lifetime filter is applied. Using a threshold for lifetime, it is now possible to emphasize long-living structures. The threshold can be chosen separately for saddles and centers to account for the different lifetime characteristics.

5 Visualization

All results in this paper are visualized in a volume spanned by two spatial coordinates and time. The extracted feature points are illustrated using spheres. The spheres are scaled and colored according to the associated lifetime, choosing a color table where high lifetime values are marked red, see Fig. 5 and 6(a). In some images, illuminated pathline segments are seeded in the extracted feature points to get a more intuitive notion of the lifetime. The pathlines are terminated after exceeding their feature lifetime, as shown in Fig. 6(b). Color-coding

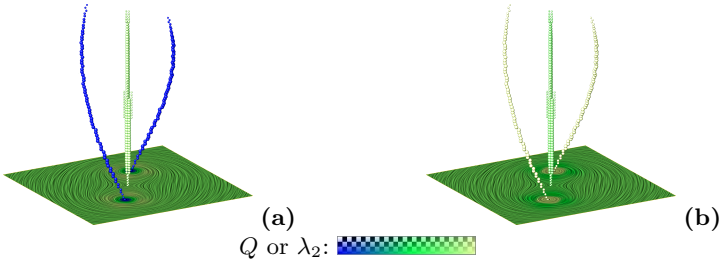

Fig. 7. Comparison of (a) λ_2 and (b) Q with the proposed Lagrangian equilibrium points. The extracted feature points include the vortex cores marked by high values of Q or low values of λ_2. In addition the saddle between the two vortices is detected.

is the same as for the spheres. The scalar fields used for the feature extraction can be added as heightfield for one time step.

To understand the local flow structure it is helpful to observe not only single pathlines but also the behavior of bundles. Such an exploratory analysis is facilitated by the possibility to select a point of interest in the LIC image. For this location, the pathline is displayed together with a moving disk depicting the flow relative to this pathline, see Fig. 2(b).

6 Results

To evaluate its effectiveness, the proposed method has been applied to two different datasets. The first dataset represents a pair of co-rotating Oseen vortices, see Fig. 5. The Oseen vortex models a line vortex that decays due to viscosity. The velocity V_Θ in the circumferential direction θ is given by

$$V_\Theta(r) = \frac{\Gamma}{2\pi} \frac{1 - e^{-(\frac{r}{r_c})^2}}{r},$$

where r is the current radius, r_c the core radius and Γ the circulation contained in the vortex. For further information, we refer to Rom-Kedar et al. [RKLW90] or Noack et al. [NMTB04]. A more complex flow field is generated by the interplay of six moving Oseen vortices, see Fig. 6. Both datasets are given for a temporal bounding box of $[-1.0, 1.0]$. The maximum lifetime window τ for integration is set to 0.3 in each direction. The extraction process takes a couple of minutes on standard hardware using non-optimized software.

For both datasets, it can be seen in Fig. 5(a) and Fig. 6(a) that the integrated acceleration is low at vortex centers and saddle points. While the lifetime is high for all features of interest in the co-rotating case, the lifetime only marks centers clearly in the complex field. The structures extracted are displayed as spheres, using the lifetime to define color and size. Due to the finite time window, the lifetime is low at the beginning, grows and then drops off to the end. After applying the lifetime filter, vortices are marked as important, but interesting saddles are also removed. This is a consequence of the fact that particles stay longer in the

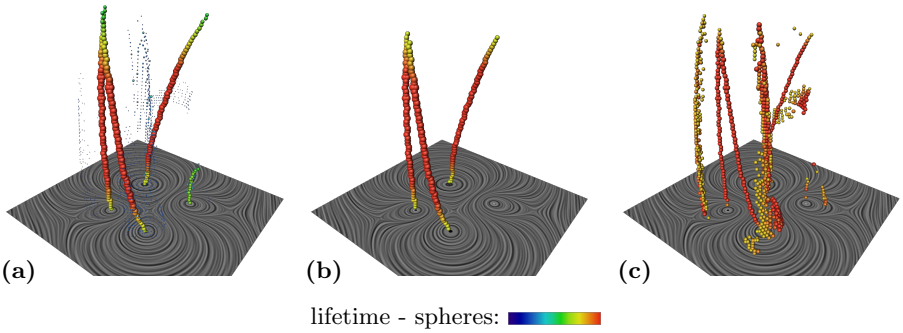

Fig. 8. Motion of six Oseen vortices: (a) All features before filtering; (b) Applying the lifetime filter filters the short-living out. (c) Employing a shorter life-time window also saddles are extracted.

vicinity of centers than in the vicinity of saddles. The illuminated pathline segments in Fig. 6(b) indicate the interval used for the integration. Pathlines seeded in vortex-like features form long centerlines due to the strong rotation within the vortex. In contrast, pathline segments seeded in saddle-like structures diverge. This is consistent with the observation that interesting saddles are removed.

Since vortex cores are extracted, Fig. 7 shows a comparison with standard vortex indicators such as λ_2 and Q. The values of λ_2 and Q are color-coded in the LIC texture and in the spheres. The minima of λ_2 or the maxima of Q reveal nearly the same structures as our approach. With λ_2 or Q, however, separating structures such as saddles cannot be extracted.

The ability of our approach to filter out short-living features is illustrated in Fig. 8. The chosen time window determines the maximal lifetime. All features with higher lifetime cannot be differentiated. Choosing a time window of length 1.0, only three long-living vortices remain.

Distinguishing between saddle and vortex regions by using the Jacobian leads to the results depicted in Fig. 8(c). In the example the lifetime for vortex-like regions is 0.6 and for saddle-like regions 0.1. With this differentiation all salient features including saddles are visible.

7 Conclusions

The proposed method enables a Galilean invariant extraction of long-living structures, based on the concept of Lagrangian equilibrium points. The method features the following characteristics, which demonstrate that the concept is a first step to overcome the limitations of standard vector field topology. The Lagrangian viewpoint helps to analyze time-dependent structures. The filtering of the extracted points by lifetime enables to mark salient structures. It provides a generalization of critical points of standard vector field topology since fixed points are also Lagrangian equilibrium points for the steady case.

In the current state, the method is still based upon two major thresholds $a_{\text{threshold}}$ and τ. While the first parameter determines whether a particle carries

a feature, the second parameter represents a characteristic feature lifetime and depends on the scale of feature lifetimes in the given dataset. Currently, the acceleration threshold is chosen heuristically. We leave it to future work to identify the relevant scale.

The application to datasets that are well understood proves the effectiveness of the proposed extraction scheme for salient structures in time-dependent flow fields. The next steps will be to improve the efficiency of the algorithm, to apply it to real world datasets, which also includes three-dimensional data, and to find ways to select appropriate parameter values automatically.

Acknowledgments

The project is part of the SFB 557 "Control of complex turbulent shear flows" and is partially supported by the DFG Emmy Noether program. The authors wish to thank George Haller, Gilead Tadmor, and Igor Mezić for fruitful discussions. All visualizations have been created using Amira - a system for advanced visual data analysis (http://amira.zib.de). The authors further want to thank the reviewers for their suggestions, which helped to improve the paper significantly.

Appendix

A transformation from one inertial frame F to another F', moving with a relative velocity $\mathbf{u}$, i.e., a Galilean transformation, is defined in space-time by $x \equiv (t, \mathbf{x}) \;\Rightarrow\; x' \equiv (t', \mathbf{x}') = (t, \mathbf{x} - \mathbf{u}t)$. The corresponding transformation for the four-velocity then is $v \equiv (1, \mathbf{v}) \;\Rightarrow\; v' \equiv (1, \mathbf{v}') = (1, \mathbf{v} - \mathbf{u})$. The differential operators $\partial_t \equiv \partial/\partial t$ and $\partial_k \equiv \partial/\partial x_k$ ($\partial_{k'} \equiv \partial/\partial x'_k$) are transformed according to $\partial_t \;\Rightarrow\; \partial_{t'} - (\mathbf{u} \cdot \nabla')$, where $\nabla \equiv (\partial_1, \partial_2, \partial_3)$ and $\nabla' \equiv (\partial_{1'}, \partial_{2'}, \partial_{3'})$ From this it is easy to see that the material derivative $D_t \equiv \partial_t + (\mathbf{v} \cdot \nabla)$ is invariant under Galilean transformations:

$$\partial_t + (\mathbf{v} \cdot \nabla) = \partial_{t'} + (\mathbf{v}' \cdot \nabla').$$

A specific consequence is that the total acceleration a flow particle experiences is Galilean invariant, $\mathbf{a} \equiv D_t \mathbf{v} = D_{t'} \mathbf{v}' \equiv \mathbf{a}'$, i.e. independent of the frame of reference.

References

[FPS+08] R. Fuchs, R. Peikert, F. Sadlo, B. Alsallakh, and E. Gröller. Delocalized unsteady vortex region detectors. In D. Saupe O. Deussen, D. Keim, editor, *VMV '08*, pages 81–90, October 2008.

[GGTH07] Ch. Garth, F. Gerhardt, X. Tricoche, and H. Hagen. Efficient computation and visualization of coherent structures in fluid flow applications. *IEEE Trans. Vis. Comput. Graph.*, 13(6):1464–1471, 2007.

[Hal01a] G. Haller. Distinguished material surfaces and coherent structures in three-dimensional fluid flows. *Physica D*, 149:248–277, 2001.

[Hal01b] G. Haller. Lagrangian structures and the rate of strain in a partition of two-dimensional turbulence. *Physics of Fluids*, 13:3365–3385, 2001.

[Hal02] G. Haller. Lagrangian coherent structures from approximate velocity data. *Physics of Fluids*, 14(6):1851–1861, 2002.

[HH89] J.L. Helman and L. Hesselink. Representation and display of vector field topology in fluid flow data sets. *Computer*, 22(8):27–36, 1989.

[HH91] J.L. Helman and L. Hesselink. Visualizing vector field topology in fluid flows. *IEEE Comput. Graph. Appl.*, 11(3):36–46, 1991.

[Hun87] J.C.R. Hunt. Vorticity and vortex dynamics in complex turbulent flows. *CSME Trans.*, 11(1):21–35, 1987.

[JH95] J. Jeong and F. Hussain. On the identification of a vortex. *Journal of Fluid Mechanics*, 285:69–94, 1995.

[LHZP07] R.S. Laramee, H. Hauser, L. Zhao, and F.H. Post. Topology-based flow visualization, the state of the art. In H. Hauser, H. Hagen, and H. Theisel, editors, *Topology-based Methods in Visualization*, pages 1–19. Springer, Berlin, 2007.

[NMTB04] B.R. Noack, I. Mezić, G. Tadmor, and A. Banaszuk. Optimal mixing in recirculation zones. *Physics of Fluids*, 16(4):867–888, 2004.

[Pan05] R. L. Panton. *Incompressible Flow*. Wiley & Sons, 2005.

[PR00] R. Peikert and M. Roth. The parallel vectors operator - a vector field visualization primitive. In *IEEE Visualization '00*, pages 263–270, 2000.

[RKLW90] V. Rom-Kedar, A. Leonard, and S. Wiggins. An analytical study of transport, mixing and chaos in an unsteady vortical flow. *Journal of Fluid Mechanics*, 214:347–394, 1990.

[Soi99] Pierre Soille. *Morphological image analysis*. Springer Berlin, 1999.

[SP00] I.A. Sadarjoen and F.H. Post. Detection, quantification, and tracking of vortices using streamline geometry. *Comput. Graph.*, 24(3):333–341, 2000.

[SP07] F. Sadlo and R. Peikert. Efficient visualization of lagrangian coherent structures by filtered AMR ridge extraction. *IEEE Trans. Vis. Comput. Graph.*, 13(6):1456–1463, 2007.

[STW+08] K. Shi, H. Theisel, T. Weinkauf, H.-C. Hege, and H.-P. Seidel. Finite-time transport structures of flow fields. In *IEEE Pacific Visualization '08*, pages 63–70, 2008.

[TP82] M. Tobak and D. Peake. Topology of three-dimensional separated flows. *Ann. Review of Fluid Mechanics*, 14:61–85, 1982.

[TWHS05] H. Theisel, T. Weinkauf, H.-C. Hege, and H.-P. Seidel. Topological methods for 2D time-dependent vector fields based on stream lines and pathlines. *IEEE Trans. Vis. Comput. Graph.*, 11(4):383–394, 2005.

[WSTH07] T. Weinkauf, J. Sahner, H. Theisel, and H.-C. Hege. Cores of swirling particle motion in unsteady flows. *IEEE Trans. Vis. Comput. Graph.*, 13(6):1759–1766, 2007.